Boreal winter stratospheric climatology in EC-EARTH: CMIP6 version

Froila M Palmeiro[1] · Javier García-Serrano[1,2] · Mario Rodrigo[1] · Marta Abalos[3] · Bo Christiansen[4] · Shuting Yang[4]

Abstract

The performance of the European Consortium Earth-system model (EC-EARTH) in the boreal winter stratosphere is comprehensively assessed for the first time, in particular its version 3.3 that contributes to CMIP6. A 100-year long simulation with prescribed climatological boundary conditions and fixed radiative forcing, representative of present-day climate, is used to evaluate the simulation of the climatological stratospheric circulation and to identify model biases. Results show that EC-EARTH has a large issue with the vertical distribution of stratospheric temperature from the tropics to midlatitudes, seemingly linked to radiative processes of ozone, leading to a biased warm middle-upper stratosphere. Associated with this model bias, EC-EARTH simulates a stronger polar vortex at upper-stratospheric levels while the Brewer-Dobson circulation at middle/lower levels is weaker than reanalysis. The amplitude of the climatological planetary waves is overall underestimated, but the magnitude of the background wave injection from the troposphere into the stratosphere is overestimated, related to a weaker polar vortex at lower-stratospheric levels and, thus, a less effective wave filtering. This bias in the westerly flow could have a contribution from parameterized waves. The overestimation of background wave driving is maximum in early-winter, and may explain the overestimated frequency of sudden stratospheric warmings at this time, as compared to reanalysis. The spatial distribution of wave injection climatology has revealed a distinctive role of the climatological planetary waves: while large-scale waves (wavenumbers 1–2) dominate the eddy heat flux over the North Pacific, small-scale waves (wavenumbers 3–4) are responsible for the doubled-lobe structure of the eddy heat flux over Eurasia. EC-EARTH properly simulates this climatological feature, although overestimates its amplitude over central Eurasia.

Keywords Stratospheric circulation · Stratospheric dynamics · Climate model bias

1 Introduction

The stratosphere is now recognized as a fundamental part of the atmosphere, not as a passive, subordinate layer of the more chaotic and variable troposphere. This recognition relies on its chemically and dynamically active role driving tropospheric variability at different timescales, including an important contribution to a wide variety of climate extremes (Domeisen and Butler 2020). This motivates a good representation of stratospheric processes in models to improve climate predictions from subseasonal to centennial timescales (see Kidston et al. 2015 for a review).

The interaction between the troposphere and the stratosphere can be schematized in vertical motions with different direction depending on the latitudinal range. In the tropics, there is a bottom-up signal dominated by upwelling, which represents upward air mass exchange, as well as vertical propagation of convection-induced waves. In the extratropics, from subtropical to subpolar latitudes, there are both a top-down component represented by downward air mass exchange and a bottom-up component linked to upward propagation of large-scale waves. Finally, most of the top-down signal occurs at polar latitudes, including

✉ Froila M Palmeiro
  fm.palmeiro@meteo.ub.edu

[1] Group of Meteorology, Universitat de Barcelona (UB), Barcelona, Spain

[2] Barcelona Supercomputing Center (BSC), Barcelona, Spain

[3] Department of Earth Physics and Astrophysics, Universidad Complutense de Madrid (UCM), Madrid, Spain

[4] Danmarks Meteorologiske Institut (DMI), Copenhagen, Denmark

downwelling and impacts associated with the stratospheric polar vortex variability. Stratosphere-troposphere coupling is of especial interest in subseasonal and seasonal climate forecasting, since the impact of the slowly varying stratosphere can be used as a predictor for tropospheric circulation beyond a week (e.g. Christiansen 2005; Sigmond et al. 2013; Domeisen et al. 2020).

The transition layer between the troposphere and the stratosphere, so-called the upper troposphere – lower stratosphere (UTLS) region, is dynamically active and modulates atmospheric composition, chemistry, and the radiation budget of the Earth (e.g. Forster and Shine 1997; Shepherd 2007). In the tropical UTLS, the troposphere and the stratosphere are well separated by the level of the lowest temperature in boreal winter, which is called the cold point tropopause (CPT). The CPT controls the amount of water vapour entering the tropical stratosphere, which is fundamental in the radiative balance (Highwood and Hoskins 1998). The main entry of chemical species to the stratosphere occurs through the tropical UTLS and constitutes the ascending branch of the meridional residual circulation, also known as the Brewer-Dobson circulation (e.g. Brewer 1949; Holton et al. 1995; Plumb 2002). This circulation can be differentiated in a shallow branch with maximum upwelling in the lower stratosphere and downwelling from subtropical to middle latitudes, and a deep branch whose upwelling extends also along the upper stratosphere and downwelling takes place from middle to polar latitudes (Plumb 2002; Birner and Bönisch 2011). Since the residual circulation is mainly wave-driven, it becomes maximum during winter, when waves can propagate into the stratosphere, and particularly in the more dynamically active Northern Hemisphere (Charney and Drazin 1961). Given the major role of the Brewer-Dobson circulation in global air mass transport, it is a key driver of changes in ozone concentration and radiative heating.

The high-latitude top-down signal is mainly characterised by the strength of the stratospheric polar vortex (Perlwitz and Graff 1995), and the largest tropospheric impact from the stratosphere is expected after extreme events: anomalous vortex intensifications (Limpasuvan et al. 2005; Baldwin et al. 2001) and primarily, sudden stratospheric warmings (SSWs; see Baldwin et al. 2021 for review). During winter, wave activity from the lower stratosphere propagates upwards through westerly background flow while increasing in amplitude until they break. This can alter the vortex strength and eventually trigger SSWs (Matsuno 1971; Charlton and Polvani 2007), although pre-existing conditions in the stratosphere also play a role in the evolution of the vortex (Chen and Robinson 1992; de la Cámara et al. 2017). In fact, the interaction between wave propagation and the background flow is a complex paradigm since

the former depends on the conditions of the latter. During winter, upward planetary wave propagation is limited by the strength of the zonal wind according to its wavenumber (Charney and Drazin 1961), and when wave breaking occurs, the deposited momentum modifies the background conditions and thus wave propagation (e.g. Matsuno 1970; Christiansen 1999; Kodera et al. 2000).

Another important phenomenon modulating the vortex variability is the Quasi-Biennial Oscillation (QBO; Baldwin et al. 2001 and references therein). The QBO is described by alternating phases of descending westerlies and easterlies from the stratopause to the lower stratosphere in the tropics, and can modulate the extratropical circulation via the Holton-Tan effect (Holton and Tan 1980). Responding to the wave propagation criteria, more waves are deflected to the pole during easterly QBO phases, so the polar vortex becomes weaker and warmer, while the opposite occurs during westerly phases (e.g. see Anstey and Shepherd 2014 for review). In addition, since both are wave-driven, there is also an expected influence of tropical upwelling on the QBO (Dunkerton 1997).

A correct representation of all these stratospheric phenomena is fundamental in global climate models (GCMs) to simulate realistic dynamics. It has been shown that biases in stratospheric processes have an impact on stratosphere-troposphere coupling (Gerber et al. 2012; Charlton-Pérez et al. 2013), tropospheric climatology (Shaw et al. 2014) and variability (Gerber et al. 2010), and constitute a source of uncertainty in future climate projections (Manzini et al. 2014). The Stratosphere-troposphere Processes And their Role in Climate (SPARC) project, part of the World Climate Research Program (WCRP), includes several initiatives to detect model biases in the stratosphere and advance towards their elimination: from the more general Dynamical Variability activity (DynVar[1]; e.g. Gerber et al. 2012) or the Network on Assessment of Predictability (SNAP[2]; e.g. Tripathi et al. 2015), to the more process-oriented QBO initiative (QBOi[3]; e.g. Butchart et al. 2018) among others.

The present study presents the first comprehensive assessment of the stratospheric climatology in the state-of-the-art EC-EARTH model and complements the study of Palmeiro et al. (2020) who reported stratospheric variability in its previous version 3.1. This model version (v3.3) is the one contributing to the Coupled Model Intercomparison Project phase 6 (CMIP6) and other international projects and initiatives, such as QBOi. The simulation analysed here, and described in Sect. 2, constitutes the control

---

[1] https://www.sparc-climate.org/activities/dynamical-variability/.

[2] https://www.sparc-climate.org/activities/assessing-predictability/.

[3] https://www.sparc-climate.org/activities/quasi-biennial-oscillation/.

simulation for the last exercise of QBOi Phase-I (i.e. ENSO experiments; Kawatani et al. in preparation) and will be the benchmark of Phase-II. The present analysis aims to contribute to a further understanding of common GCM biases in the stratosphere, and to serve as a reference for future multi-model analyses where EC-EARTH will be taking part.

2 Model, simulation, and methods

This study focuses on the atmospheric component of the European Consortium coupled climate model EC-EARTH, which is based on the Integrated Forecast System (IFS) atmosphere model of the European Centre for Medium-Range Weather Forecasts (ECMWF). Details about the other main components of the CMIP6 version of EC-EARTH – *EC-EARTH3.3*, i.e. ocean (Nucleus for European Modelling of the Ocean - NEMO3.6), land (Hydrology Tiled Scheme for Surface Exchanges over Land – H-TESSEL) and sea-ice (Louvain-la-Neuve Sea Ice Model – LIM3), as well as the coupler (Ocean Atmosphere Sea Ice Soil – OASIS3-MCT), can be found in Haarsma et al. (2020; developed for HighResMIP) and Döscher et al. (2022). The standard configuration of IFS in EC-EARTH3.3, based on cycle 36r4, is at horizontal spectral resolution T255 (triangular truncation at wavenumber 255), corresponding approximately to 0.7° in longitude-latitude (~80 km), with 91 vertical levels up to 0.01 hPa (L91); hence, the model is considered as "high top". For comparison, the standard configuration of IFS in the CMIP5 version of EC-EARTH – *EC-EARTH2.3* (Hazeleger et al. 2010, 2012), based on cycle 31r1, was at T159, approximately 1.125° in longitude-latitude (~125 km), with 62 vertical levels up to 5 hPa; thus, considered as a "low top" model. Developed at ECMWF as a weather model, IFS is tuned and improved for climate purposes by the EC-Earth Consortium (see Döscher et al. 2022 for review). Examples of major advances from CMIP5 to CMIP6 follow. While EC-EARTH2.3 only accounted for the direct effects of prescribed aerosol concentration, EC-EARTH3.3 also includes a representation of the indirect effects via the aerosol impact on clouds (see Wyser et al. 2020 for details). Note that interactive chemistry (particularly, stratospheric chemistry) is not yet implemented in the standard configuration of EC-EARTH (van Noije et al. 2021); so there is no coupling between chemistry and model dynamics/physics. Now, EC-EARTH includes a non-orographic gravity wave (NGW) parameterization, formulated by Scinocca (2003), which, in contrast to previous IFS cycles (before 35r3) that used Rayleigh friction, can spontaneously generate QBO-like variability (e.g. Christiansen et al. 2016); this NGW parameterization consists of a zonally-symmetric momentum flux that is continuously launched from the mid-troposphere to simulate the effect of gravity waves, and it has been modified from the original implementation in cycle 36r4 (Orr et al. 2010) to be resolution-dependent (see Davini et al. 2017 for details). Orographic gravity waves are parameterized following Lott and Miller (1997) for blocking and hydrostatic gravity wave drag and Beljaars et al. (2004) for turbulent orographic form drag (see ECMWF 2010 for details). Although Döscher et al. (2022) provide information of how stratospheric composition and chemistry are configured in EC-EARTH3.3, neither dynamics nor climatological aspects of the stratospheric circulation are reported. At present this gap calls for attention now that the stratosphere is properly resolved in EC-EARTH.

EC-EARTH3.3 contributes to most CMIP6-endorsed MIPs[4], particularly relevant here – the Dynamics and Variability MIP (Gerber and Manzini 2016) and the Polar Amplification MIP (Smith et al. 2019), but it also participates in other international initiatives such as the Multi-Model Large Ensemble Archive (Deser et al. 2020) or the SPARC's QBOi. With the focus on the model performance of stratospheric climatology, we make use of the time-slice "Experiment 2" from QBOi phase-I. It consists in a 100-year long atmosphere-only simulation with prescribed, repeated seasonal cycle for sea surface temperature (SST) and sea ice concentration (SIC), whose climatology is computed over 1988–2007, and fixed radiative forcing, aerosols and chemical constituents (including ozone) at year 2002, which is well removed from any explosive volcanic eruption and ENSO was in a neutral phase; hence, there is no interannual variability or secular change in the applied forcings (see Butchart et al. 2018). Note that both boundary conditions and radiative forcing/atmospheric composition are taken from the CMIP6 input dataset, instead of CMIP5 as in the original QBOi protocol. Also, it is worth noting that this "Experiment 2" represents the *control* simulation of the QBOi El Niño/La Niña sensitivity experiments (Kawatani et al., in preparation).

Outputs from QBOi simulations are stored at JASMIN, provided by the British Atmospheric Data Centre (BADC). Here, monthly means of zonal wind (u), air temperature (T) and geopotential height at 28 pressure levels from 1000 to 1 hPa are analysed. Daily-mean variables are only available in a subset of pressure levels; here 300, 250, 200, 100, 70, 50, 30, 20 and 10 hPa are analysed. The latter have been used to compute the residual (mass) streamfunction in the Transformed Eulerian-Mean (TEM) framework, which in pressure coordinates can be defined as follows (e.g. Andrews et al. 1987; Abalos et al. 2015):

---

[4] http://www.ec-earth.org/cmip6/ec-earth-in-cmip6/.

$$\Psi^* = \frac{a\cos\phi}{g}\int_0^p [v]\, dp + \frac{a\cos\phi}{g}\frac{p}{HS}[v^*T^*]$$

where a is the Earth radius, ϕ is latitude, g is the gravity, p is pressure, H is the scale-height (7 km), and $S = HN^2/R$ is the stability parameter, with N^2 the squared Brunt-Väisälä frequency and R the gas constant for dry air ($287 m^2/s^2 K$). $[v]$ is the Eulerian-mean meridional wind and $[v^*T^*]$ the eddy heat flux, where $*$ indicates perturbation from the zonal-mean and $[]$ denotes a zonal-mean. Note that $[v^*T^*]$ is proportional to the vertical component of the Eliassen-Palm flux, thereby related to vertical propagation of wave activity (e.g. Andrews et al. 1987; Vallis 2017).

The analysis is focused on boreal winter, namely December-February (DJF). When indicated, the model performance is compared to ERA-Interim reanalysis (Dee et al. 2011) covering the period 1979–2019. The statistical significance of the model biases is assessed with a Student's t-test for equal means at 95% confidence level considering each winter as an independent sample.

3 Results

3.1 Zonal-mean structure

Figure 1 shows vertical cross-sections of zonal-mean zonal wind (left column) and temperature (right column) in boreal winter, illustrating that EC-EARTH (first row) properly simulates the main features of the observed circulation (ERA-Interim; second row); although clear model biases are present (bottom row). In the troposphere, the subtropical jet is slightly shifted to the north (Fig. 1e). In the stratosphere, which is the target of the study, there are two different behaviours. EC-EARTH largely overestimates the climatological westerly wind at upper-stratospheric midlatitudes, where the core of the polar vortex is stronger (~ 6 m/s) and shifted poleward as compared to reanalysis (Fig. 1, left column). Linked to this bias, the meridional extension of the warm tropical stratopause is also biased towards higher latitudes (~ 6 K; Fig. 1, right column). On the other hand, EC-EARTH underestimates the climatological westerly wind (~ 3 m/s) in the lower stratosphere at polar latitudes (Fig. 1e), consistent with a warm bias (~ 2-4 K; Fig. 1f) in thermal wind balance. The model bias in the strength of the polar vortex at these low levels may affect the vertical propagation of planetary-scale waves from the troposphere into the stratosphere.

The most striking aspect of the model bias in zonal-mean temperature is probably at low latitudes (Fig. 1f). There appears to be an important issue with the vertical distribution of tropical stratospheric temperature, with a warm bias
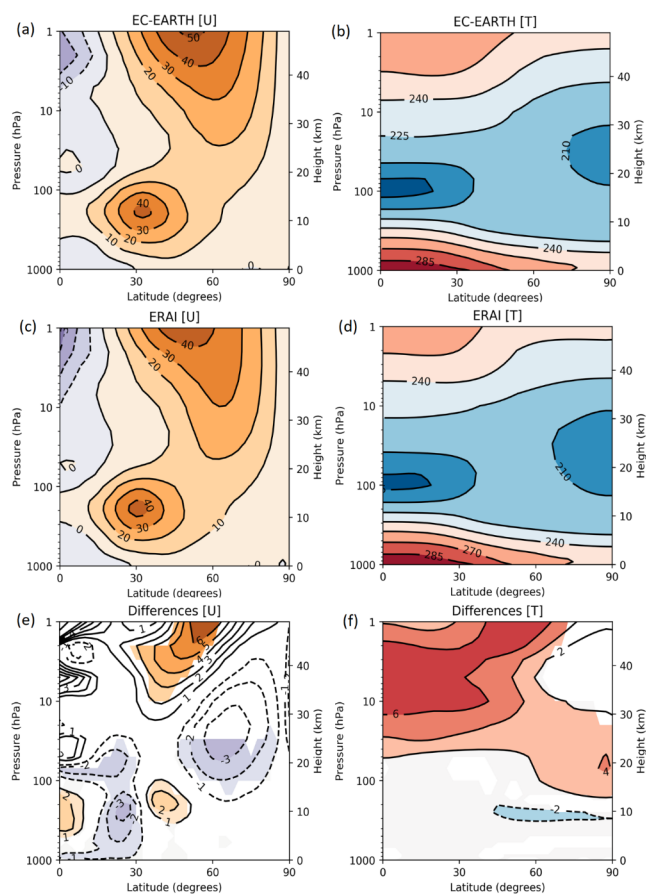

Fig. 1 Vertical cross-section of DJF zonal-mean zonal wind (left; m/s) and temperature (right; K) climatology in EC-EARTH (top row) and ERA-Interim (middle row), and its difference (bottom row). Statistically significant areas at 95% confidence level are shaded in panels **e,f**

of ~ 6 K at middle-upper levels. Note that this thermal bias is persistent throughout the seasonal cycle (see Supplementary Material). The temperature in the stratosphere mainly relies on radiative process (e.g. Vallis 2017), hence it is likely due to a problem with the heating linked to ozone absorption between 20 and 50 km (e.g. Edwards 1982), as reported previously for ECMWF-IFS (Hogan et al. 2017). To discard any possible effect of comparing a simulation with fixed radiative forcing (see Sect. 2) against the ERA-Interim reanalysis with time-varying radiative forcing, the model bias has also been assessed using CMIP6 AMIP runs (Fig. 11 in Appendix 3), which shows the same issue with the tropical stratospheric temperature. Note that the differences in ozone concentration between EC-EARTH, prescribed from CMIP6 input dataset, and ERA-Interim climatology are minor and inconsistent with the warm bias in Fig. 1f (see Supplementary Material), pointing at the ozone radiation scheme as the cause of the model systematic error (see discussion in Sect. 4).

3.2 Horizontal and meridional circulation

3.2.1 Polar vortex

In the extratropical stratosphere, vertical motions are relatively slow (much slower than in the troposphere), the stratification is high and the Rossby number small, thereby the circulation is well described by quasi-geostrophic approximation and the flow can be considered of large-scale and quasi-horizontal (see Andrews et al. 1987, Vallis 2017 for a review on geostrophic scaling). To better characterise the model bias in zonal wind (Fig. 1e), Fig. 2 shows longitude-latitude maps at three vertical levels: 100 hPa (bottom), 30 hPa (middle) and 3 hPa (top); representative of the lower, middle and upper stratosphere, respectively.

At 100 hPa, reminiscent of the upper-tropospheric circulation (Fig. 2 g,h), EC-EARTH depicts a strengthening (weakening) at the poleward (equatorward) side along the North African-Asian jet and in the North Pacific (Fig. 2i), implying a northward shift of the subtropical jet as compared to ERA-Interim, which is consistent with the zonal-mean analysis (Fig. 1e). In the North Atlantic, instead, EC-EARTH yields a weaker and, particularly, less tilted eddy-driven jet than reanalysis (Fig. 2i), a common bias in GCMs (e.g. CMIP3 - Woollings and Blackburn 2012; CMIP5 - Zappa et al. 2013; CMIP6 - Simpson et al. 2020).

At 30 hPa, the climatological flow encircles hemispherically at higher latitudes (Fig. 2d,e). The model underestimation of the polar vortex strength (Fig. 1e) is apparent over both the Eurasian and northern North Pacific regions (Fig. 2f). At 3 hPa, the climatological westerly wind is stronger (Fig. 2a,b), and the model overestimation of the polar vortex strength at midlatitudes is especially noticeable over the eastern North Pacific and the North Atlantic-European region.

3.2.2 Brewer-Dobson circulation

The Brewer-Dobson circulation is a meridional overturning, residual mass circulation in the stratosphere that transports air from the tropical tropopause, linked to tropical upwelling, towards extratropical latitudes, including polar downwelling (see Shepherd 2007 for review). Due to limited availability of daily data (see Sect. 2), the analysis can only assess the Brewer-Dobson circulation at middle and lower levels. EC-EARTH properly simulates the observed upward and downward motions of the meridional circulation (Fig. 3a,b), although model biases are found. In particular, the strength of the residual circulation is underestimated from low to midlatitudes and overestimated at subpolar latitudes (Fig. 3c). Separating the residual streamfunction into the Eulerian-mean component (Fig. 3, middle row) and

Fig. 2 DJF climatology of zonal wind at 100 hPa (bottom row), 30 hPa (middle row) and 3 hPa (top row) in EC-EARTH (left; **a,d,g**) and ERA-Interim (middle; **b,e,h**), and its difference (right; **c,f,i**). Statistically significant areas at 95% confidence level are shaded in panels **c,f,i**
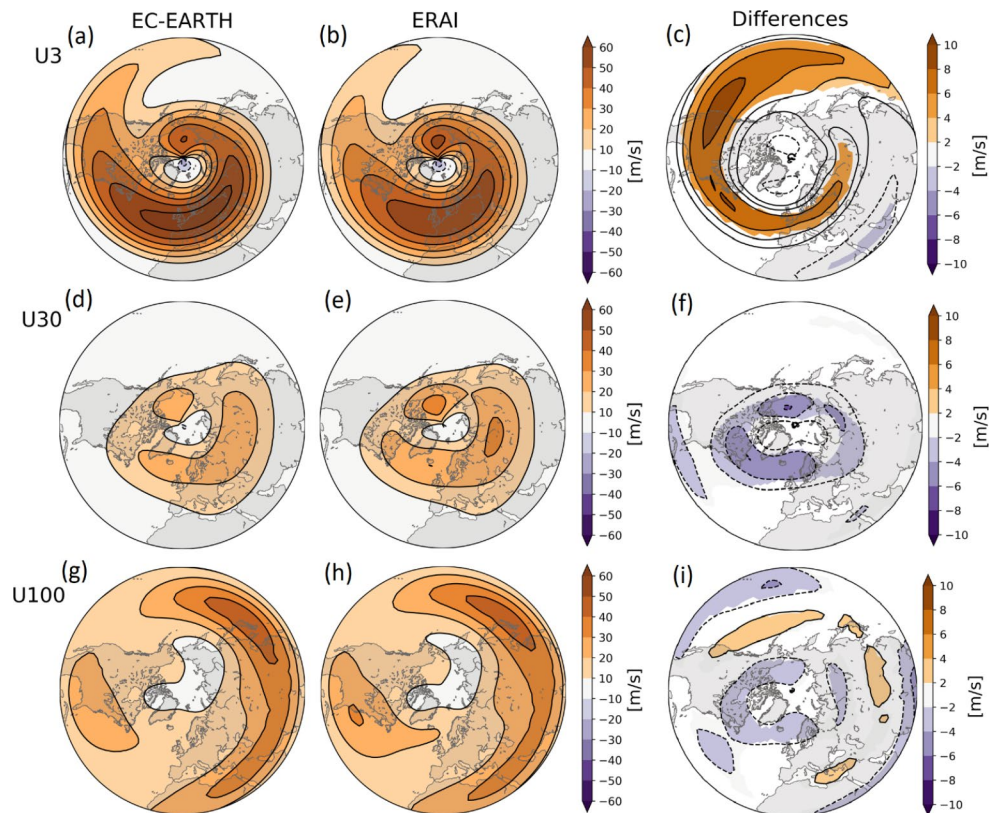
Fig. 3 DJF climatology of the residual streamfunction (top row; divided by a, kg/m·s), its Eulerian-mean component (middle row; see Sect. 2), and zonal-mean meridional wind (bottom row; m/s) in EC-EARTH (left; **a,d,g**) and ERA-Interim (middle; **b,e,h**), and its difference (right; **c,f,i**). Note the irregular contours in panels **a,b,d,e** ($\pm 200, \pm 150, \pm 100, \pm 75, \pm 50, \pm 30, \pm 20, \pm 10, \pm 5, \pm 3, \pm 1$) and **c,f** ($\pm 100, \pm 50, \pm 30, \pm 10, \pm 5, \pm 3, \pm 1$); the dotted contours in panels **g,h** correspond to ± 0.1 m/s. Statistically significant areas at 95% confidence level are shaded in panels **c,f,i**
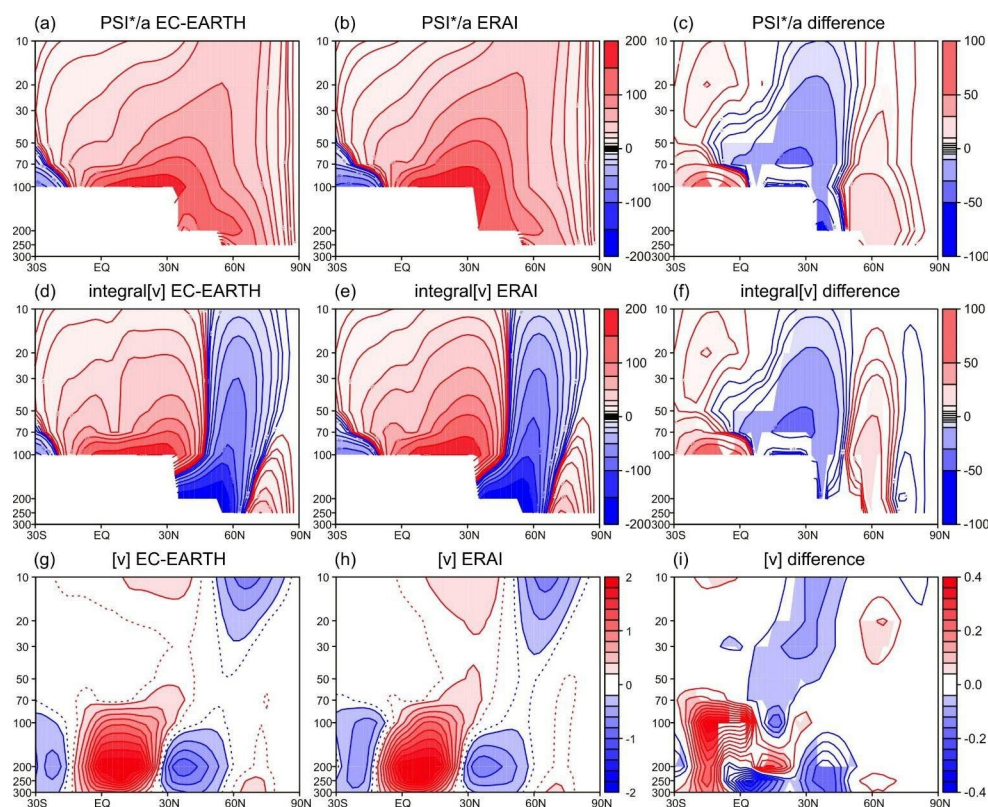
the eddy component (not shown), reveals that the former dominates the model bias (Fig. 3f): both, the direct cell in the tropical-subtropical stratosphere and the indirect cell at mid-latitudes are weaker than in reanalysis (Fig. 3d,e). The model bias can be traced back to an underestimation of the zonal-mean meridional wind ([v]; Fig. 3 g,h), particularly the poleward flow in the subtropics, with negative difference values from 10 hPa to the tropopause (Fig. 3i). Note that EC-EARTH also shows a marked bias of the divergent flow in the equatorial upper troposphere–lower stratosphere (Fig. 3c,f,i). These biases in the Brewer-Dobson circulation are consistent with the biases in temperature as discussed below (Sect. 4).

Figure 4 displays the zonal-mean eddy heat flux, [v*T*], which is the main contribution to the eddy component of the residual streamfunction (see Sect. 2) and is proportional to the vertical component of the Eliassen-Palm flux, thus indicative of vertical wave propagation (e.g. Andrews et al. 1987). EC-EARTH accurately simulates the magnitude and extension of [v*T*] in the lower-middle stratosphere (Fig. 4a,b). It shows a slight northward shift from 50 to 10 hPa, as compared to reanalysis (Fig. 4c), but is not statistically significant due to the large variability at those levels. EC-EARTH overestimates the eddy heat flux around 100 hPa at high latitudes, which may counteract the Eulerian-mean component of the meridional circulation (Fig. 3f), contributing to the biased downwelling (Fig. 3c). There is also a positive model bias in the upper-tropospheric mid-latitudes (Fig. 4c), consistent with the biased jetstream (Fig. 1e).

3.3 Wave activity

The total wave injection from the troposphere into the stratosphere is estimated as the zonally-averaged 100 hPa

Fig. 4 DJF climatology of zonal-mean eddy heat flux ([v*T*]; m·K/s) in **a** EC-EARTH and **b** ERA-Interim, and its difference (**c**). Statistically significant areas at 95% confidence level are shaded in panel **c**
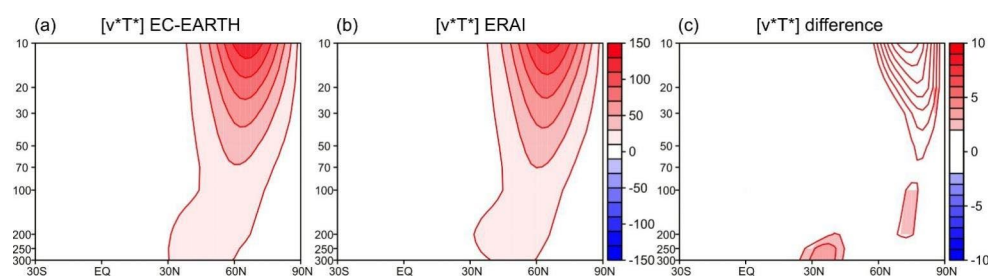
v*T* over 45-75 N (Fig. 5a; e.g. Nishii et al. 2009; Smith and Kushner 2012), and compared to its high-latitude contribution averaged over 60-75 N (Fig. 5b); the latter is also considered because stratospheric planetary-scale wave propagation maximizes at high latitudes (Shaw and Perlwitz 2013; Dunn-Sigouin and Shaw 2015, 2018). The seasonal cycle of the climatological wave activity flux is overall well simulated by EC-EARTH (blue line), although it is overestimated, as compared to reanalysis (black line), in early winter, December/mid-January, and slightly underestimated in late winter, mid-January/February (Fig. 5a). The former appears to be associated with an overestimation of the high-latitude eddy heat flux (Fig. 5b), in agreement with the analysis of [v*T*] (Fig. 4c). This overestimation of the climatological wave activity in early winter could explain the higher frequency of SSW occurrence in the model at this time of the year (see Fig. 9 in Appendix 1), given the potential relationship between the seasonality of these two fields (Palmeiro et al. 2020).

Figure 6 shows the climatology of v*T*, whose spatial distribution depicts the key regions of tropospheric wave driving, linked to the climatological stationary wave pattern (e.g. Plumb 1985): poleward warm air advection over eastern Eurasia-northwestern North Pacific and equatorward cold air advection over central Eurasia-northeastern Europe; note a weak southward advection of warmer air over northern Canada (e.g. Newman and Nash 2000). EC-EARTH correctly simulates the two areas contributing to positive zonal-mean eddy heat flux (Fig. 6a,b; cf. Figures 4a and b and 5a), although some differences are found (Fig. 6c). In particular, while the model simulates a weaker and eastward-shifted centre of action around the Aleutian Islands, it yields a weaker but westward-shifted centre of action in the North Atlantic-European sector. On the other hand, EC-EARTH overestimates the amplitude of v*T* over central Eurasia (Fig. 6c).

Decomposing the eddy heat flux into wavenumbers (WNs; Fig. 7) provides valuable information on the waves that contribute to the wave injection. Long planetary-scale waves (WN1 and WN2) are associated with most of the climatological v*T* over the North Pacific and Eurasia (Fig. 7a,b), and represent the largest contributors to the model bias around the Aleutian Islands (Fig. 7c). Interestingly, WN3 contributes to the amplitude of the wave driving in the North Pacific sector (Fig. 7d,e) and shapes the tilt of the model bias toward lower latitudes (Fig. 7f). WN3 appears also to elongate the centre of action of the climatological eddy heat flux over Eurasia (Fig. 7d,e), better defining the shift bias in the North Atlantic and the amplitude bias over central Eurasia (Fig. 7f). On its part, WN4 seems to be the key contributor to the characteristic double lobe of the wave injection over Eurasia, with maxima over
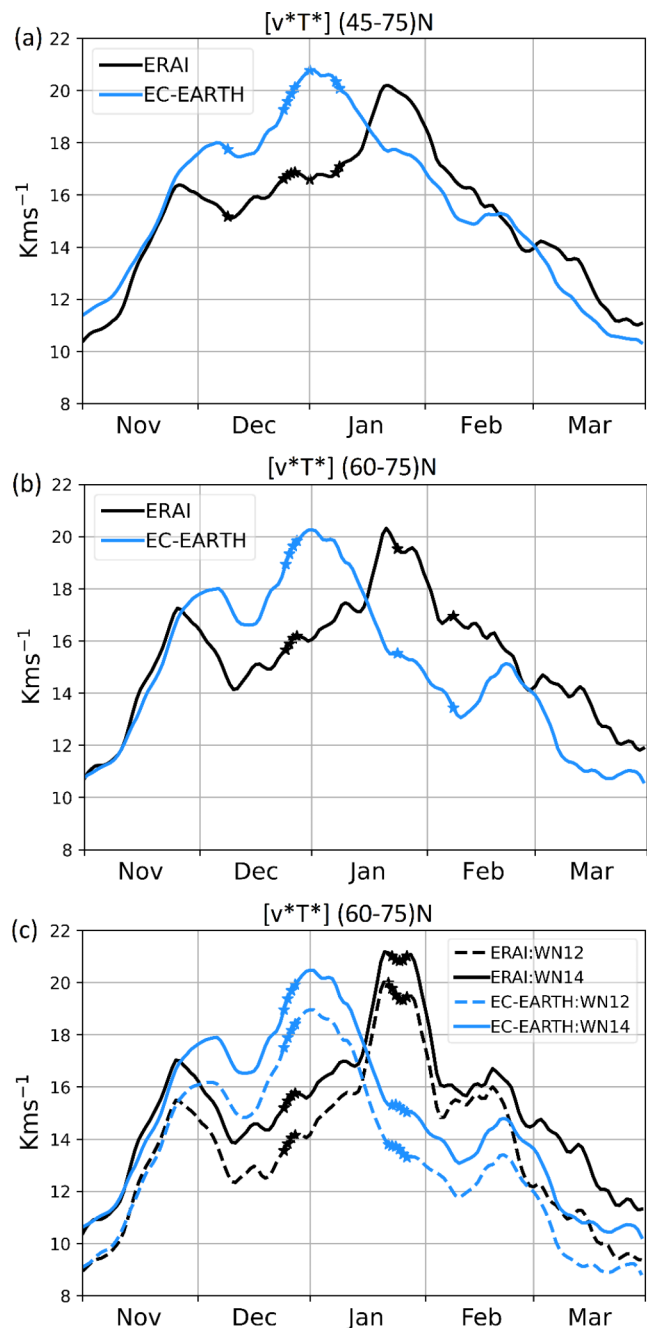
Fig. 5 Daily climatology of 100-hPa zonal-mean eddy heat flux ($[v*T*]$; m·K/s) averaged over 45-75 N (**a**) and 60-75 N (**b**) in EC-EARTH (blue) and ERA-Interim (black). The high-latitude eddy heat flux has been decomposed into WN1-2 (dashed) and WN1-4 (solid) in panel **c**. Time-series are smoothed with a 7-day running-mean. Statistically significant differences at 95% confidence level are indicated with stars in both time-series

Scandinavia and Siberia (cf. Figure 7 g,h, Fig. 6a,b). Note that both large-scale waves (WN1-2) and small-scale waves (WN3-4) contribute to the EC-EARTH overestimation of the wave forcing in early winter (Fig. 5c). WN5 mainly adds to the model overestimation of v*T* climatology at

Fig. 6 DJF climatology of 100-hPa eddy heat flux (v^*T^*; m·K/s) in **a** EC-EARTH and **b** ERA-Interim, and its difference (**c**). Statistically significant areas at 95% confidence level are shaded in panel **c**
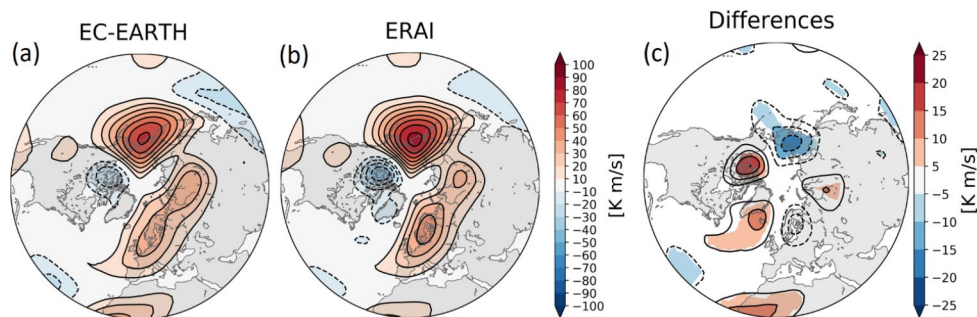
Fig. 7 As Fig. 6, but after decomposing v^* and T^* into wavenumbers (WNs): 1–2 (**a-c**), 1–3 (**d-f**), 1–4 (**g-i**) and 1–5 (**j-l**). Statistically significant areas at 95% confidence level are shaded in panels **c,f,i,l**
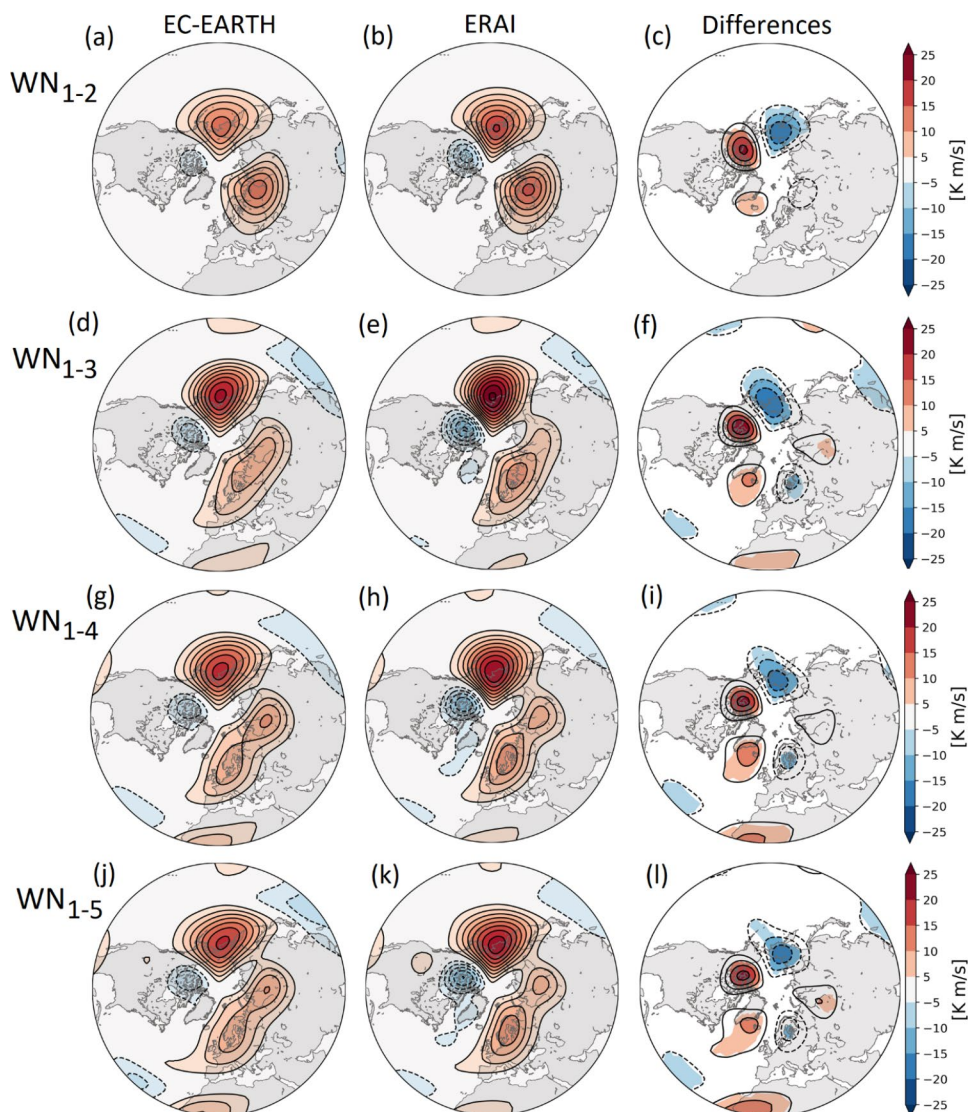
100 hPa over central Eurasia (Fig. 7 L), although its contribution to the stratospheric circulation is expected to be minor due to the Charney-Drazin wave filtering in the vertical propagation.

Finally, the vertical structure of the climatological stationary waves is assessed. Figure 8 shows zonal-mean deviations of the geopotential height field decomposed into wavenumbers. More evident for large-scale waves (WN1, WN2; first, second row) than for small-scale waves (WN3, WN4; third, fourth row), they all depict a westward tilt with height associated with upward vertical propagation (e.g. Andrews et al. 1987). In the stratosphere, WN1 is the

Fig. 8 Longitude-pressure cross-section of DJF geopotential height (m) climatology in EC-EARTH (left) and ERA-Interim (middle), and its difference (right), decomposed into wavenumbers (WNs): 1 (**a-c**), 2 (**d-f**), 3 (**g-i**) and 4 (**j-l**). Statistically significant areas at 95% confidence level are shaded in panels **c,f,i,l**
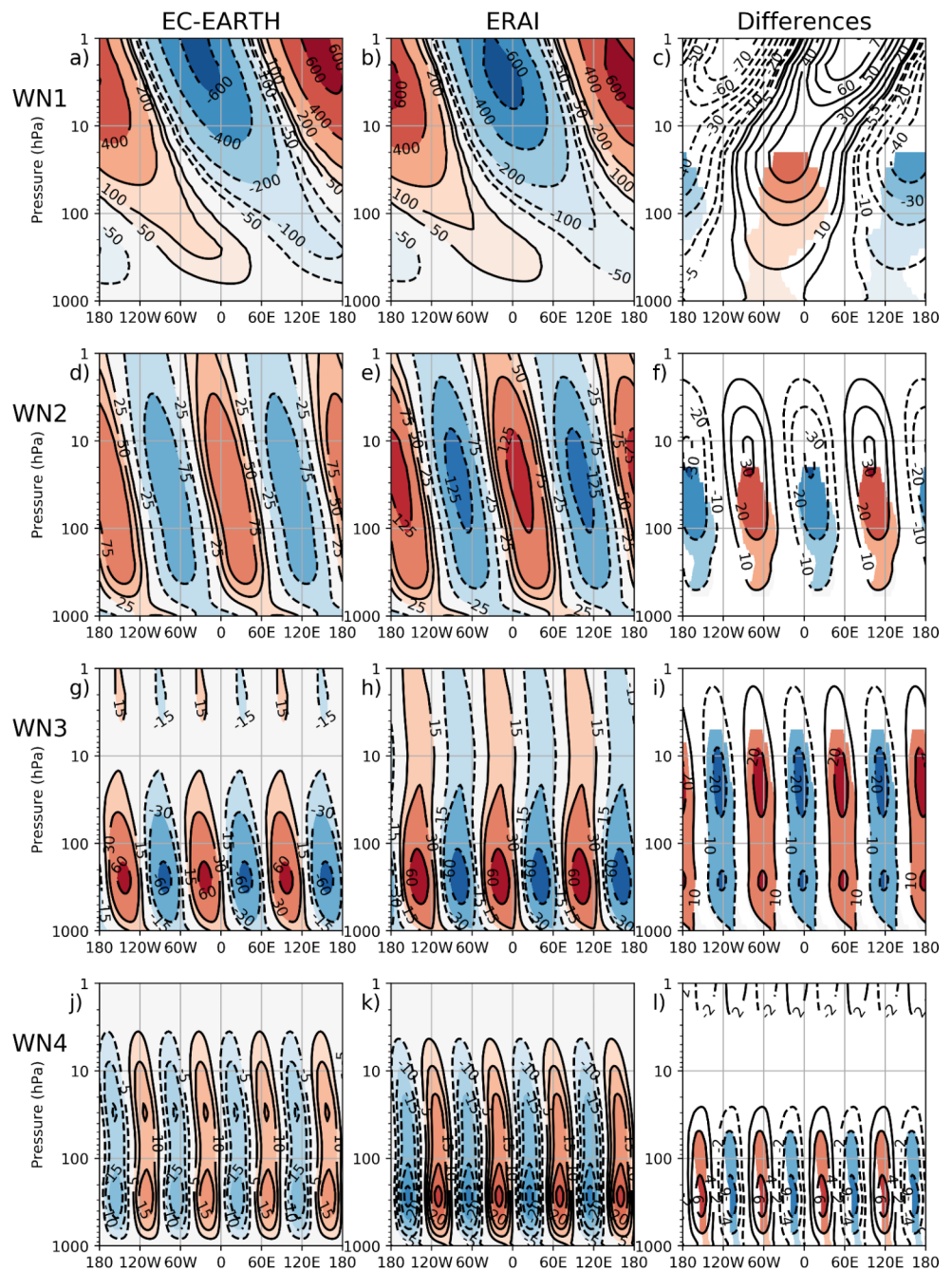
only wave that EC-EARTH simulates with correct amplitude (Fig. 8a,b), yet weaker than ERA-Interim (Fig. 8c). Compared to reanalysis, the model systematically underestimates the amplitude of WN2 (Fig. 8d,e), WN3 (Fig. 8 g,h) and WN4 (Fig. 8j,k).

A close inspection to climatological WN1 (Fig. 8a,b), where the positive zonal-eddy component projects on the stratospheric Aleutian High and the negative one on the displaced polar vortex (e.g. Nigam and DeWeaver 2003) forming a couplet that propagates into the mesosphere (Harvey and Hitchman 1996; Harvey et al. 2002), reveals

that EC-EARTH simulates it with a westward shift in the upper stratosphere, which leads to an apparent (but not statistically significant) turning of the vertical tilt (Fig. 8c). On the contrary, the model bias in the lower stratosphere displays a statistically significant eastward shift (Fig. 8, first row), which is consistent with the eastward shift of v*T* around the Aleutian Islands noted above (Figs. 6c and 7c).

The model bias of WN2 mainly relies on an amplitude underestimation in the lower stratosphere (Fig. 8f). The wrong performance of WN3's amplitude is maximum in

the lowermost stratosphere (~200 hPa) and below the middle stratosphere (Fig. 8i). The amplitude underestimation of WN4 is restricted to the lower-lowermost stratosphere (Fig. 8 L).

4 Summary and conclusions

This study presents the first comprehensive assessment of boreal winter stratospheric climatology in EC-EARTH, particularly version 3.3 that contributes to CMIP6 and SPARC's Quasi-Biennial Oscillation initiative (QBOi). Indeed, the simulation reported here corresponds to the 100-year control "Experiment 2" of QBOi with prescribed climatological SST and SIC over 1988–2007 and fixed radiative forcing at year 2002; note that the boundary conditions (taken from AMIP) and the radiative forcings are from CMIP6, not from CMIP5 as in the original QBOi protocol (Butchart et al. 2018). Boreal winter stratospheric variability in EC-EARTH was comprehensively assessed by Palmeiro et al. (2020), although with a previous version of the model, EC-EARTH3.1. Appendices 1 (Figs. 9) and 2 (Fig. 10) report the EC-EARTH3.3 performance of the key stratospheric variability phenomena in this simulation, i.e. sudden stratospheric warmings (SSWs) and the QBO, that are overall realistic. Richter et al. (2020) provide QBO metrics for EC-EARTH3.3 in a CMIP6 multi-model analysis. The modulation of the QBO in EC-EARTH3.3 (Fig. 10) by El Niño and La Niña is currently under investigation in the framework of QBOi (Christiansen et al., Kawatani et al.; in preparation). On the other hand, the influence of El Niño/La Niña on SSWs in a previous version of the model, EC-EARTH3.2, has been recently assessed (Palmeiro et al. 2022). Also, inspired by the preliminary results of Haarsma et al. (2020), there are ongoing efforts in the EC-Earth consortium to address the impact of horizontal resolution and radiative forcing on SSWs in the CMIP6 version of the model reported here. In the following, we summarize our main findings on the model climatology in the stratosphere, which may affect variability and predictability (e.g. Hogan et al. 2017; Polichtchouk et al. 2019).

EC-EARTH shows a large issue with the vertical distribution of zonal-mean stratospheric temperature from the tropics to mid-latitudes, associated with a biased warm middle-upper stratosphere (~6 K; Fig. 1f). Linked to the enhanced meridional temperature gradient, and in thermal wind balance, the model simulates a stronger and northward-shifted core of the polar vortex at upper-stratospheric mid-latitudes, as compared to reanalysis ([u]; Fig. 1e). This issue with the zonal-mean temperature appears related to ozone heating rate and can be alleviated by modifying the ozone radiation scheme (e.g. timestep, zenith angle, diurnal

cycle), according to recent progress with ECMWF-IFS (Hogan et al. 2017; Shepherd et al. 2018), which will be incorporated in the next generation of EC-EARTH (version 4) as it will use IFS cycle 43r3 where these improvements became operational. The model bias in the low-latitude stratospheric temperature has also an impact on the zonal-mean meridional wind ([v]; Fig. 3i) via the Coriolis term of the momentum equation in the meridional direction, that involves [u]. In particular, positively biased [u] is associated with a weaker [v] in the subtropical low-to-middle stratosphere, which in turn leads to a weaker Brewer-Dobson circulation (Fig. 3c,f). While the residual circulation is mainly driven by the torque induced by wave dissipation, recent work has highlighted the important role of anomalous heating in forcing changes in the Brewer-Dobson circulation (Ming et al. 2016). We argue that this mechanism could be contributing to the residual circulation bias in EC-EARTH. Indeed, the negative bias in tropical upwelling throughout the low-to-middle stratosphere is consistent with the positive bias in the background static stability (Fig. 1f), linked to the biased radiative heating by ozone absorption (as shown for ECMWF-IFS; Hogan and Bozzo 2018), via the TEM thermodynamic equation (e.g. Andrews et al. 1987). On the other hand, resolved wave drag does not feature large biases (see small eddy heat flux bias in Fig. 4c), but parameterized wave drag could contribute to the bias in residual circulation. This contribution might be assessed in EC-EARTH4 (CMIP7), which will presumably have a much weaker thermal bias linked to ozone heating rate.

EC-EARTH also shows a warm bias in the lower stratosphere over the polar cap (Fig. 1f), but, in this case, it does not appear related to radiative processes of ozone (Hogan et al. 2017; Shepherd et al. 2018). Associated with this positive temperature bias, the model simulates a stronger downwelling (Fig. 3c) and a weaker westerly wind of the polar vortex at lower-stratospheric high-latitudes (Fig. 1e), which suggests it is a consequence of too-strong wave driving - resolved (see below) and parameterized (see Appendix 4). EC-EARTH presents a polar cold bias in the lowermost stratosphere (~200 hPa; Fig. 1f), a common problem in GCMs that is related to an excessive transport of water vapour from the troposphere and its infrared thermal emission (Gates et al. 1999; Stenke et al. 2008; Hogan et al. 2017), leading to a biased subtropical upper-tropospheric jetstream (Fig. 1e); but this is out of scope.

The amplitude of the climatological planetary waves in the stratosphere is overall underestimated by EC-EARTH at lower levels (~10–200 hPa; Fig. 8), but the magnitude of the background wave injection from the troposphere into the stratosphere (i.e. hemispheric-average 100-hPa v*T*) is overestimated (Fig. 4c), particularly in early winter – December-January (Fig. 5). This behaviour could be

explained by the negative model bias in zonal-mean zonal wind in the lower stratosphere ([u]; Fig. 1e), since a weaker westerly flow is less effective for the Charney-Drazin wave filtering in the vertical propagation. A contributor to this bias could be the parameterized non-orographic gravity wave driving that might be excessive in this model version (see Appendix 4) and can induce changes in the mean flow (de la Cámara and Lott 2015). Further, the overestimated background wave injection could be linked to the overestimated occurrence of SSWs in early winter (Fig. 9), according to its potential impact on the SSW seasonal cycle (e.g. Palmeiro et al. 2020). Hence, attention is needed in model validation to assess the simulation of realistic climatological eddy heat flux seasonality.

The analysis of the spatial distribution of v*T* climatology has brought new insight into the role of climatological planetary waves on the background wave injection. While large-scale waves (WN1-2) dominate the eddy heat flux over the northern North Pacific, small-scale waves (WN3-4) are responsible for the distinctive doubled-lobe structure of the eddy heat flux over Eurasia (Fig. 7). EC-EARTH properly simulates this climatological feature, although overestimates its amplitude over central Eurasia (Fig. 6c). Small-scale planetary wave activity over Eurasia is prominent during wintertime, at seasonal (e.g. Liu et al. 2014; Smoliak and Wallace 2015), intraseasonal (e.g. Bueh and Nakamura 2007; García-Serrano et al. 2017) and sub-monthly (e.g. Palmeiro et al. 2020, 2022) timescales. It is also worth stressing that small-scale planetary waves propagate vertically reaching middle-upper stratospheric levels (Fig. 8), in agreement with the teleconnection pathway of Eurasian wave activity and the NAO via changes in the polar vortex strength (e.g. Kuroda and Kodera 1999; Takaya and Nakamura 2008).

Recommendations also emerge from this study. Although EC-EARTH spontaneously simulates QBO-like variability, its NGW parameterization follows a source-unrelated approach (see Sect. 2). The absence of source mechanisms in NGW parameterizations limits their potential calibration with the growing number of in-situ and satellite observations and is a cause of systematic errors (de la Cámara et al. 2016). Implementing a source-related parameterization, where the amplitude of NGWs depends on the resolved dynamics in the model, may help to reduce biases in the tropical and extratropical stratospheric climatology and variability (Berner et al. 2017). Another way to alleviate systematic errors in EC-EARTH may be to add chemistry coupling, thereby providing a suitable link between chemical reactions and stratospheric temperature and circulation via the radiative heating associated with the constituents. It has been shown that chemistry-climate models substantially reduce biases in stratospheric transport, climatology and

variability (Hardiman et al. 2017; Haase and Matthes 2019). Implementing fully-interactive stratospheric chemistry is indeed one of the current strategies in climate modelling (Collins et al. 2017; Morgenstern et al. 2017).

A prospect note follows. Good representation of stratospheric circulation and stratosphere-troposphere coupling is expected to provide predictability in subseasonal and seasonal climate forecasting, and careful assessments of the dynamics involved in stratospheric variability of GCM-based forecast systems are underway, e.g. in the tropical stratosphere (Stockdale et al. 2022) and in the polar stratosphere (Portal et al. 2022). The results shown here recommend that the dynamics involved in stratospheric climatology should also be assessed in forecast mode, for example in the Eulerian-mean [u] (linked to extratropical wave driving) and [v] (related to the Brewer-Dobson circulation), since biases may affect predictions once the models are initialised (see Saurral et al. 2021).

5 Appendix

5.1 Appendix 1. SSWs in EC-EARTH3.3

See Fig. 9
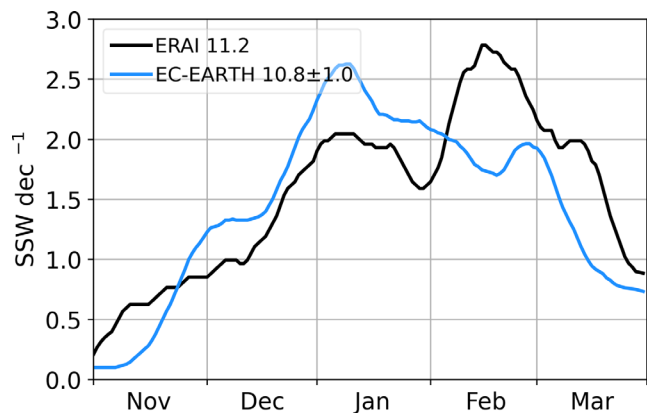
Fig. 9 November to March climatological distribution of SSWs per decade in a [-10,10]-day window around the SSW date in EC-EARTH (blue) and ERA-Interim (black). Time-series are smoothed with a 7-day running-mean. Note that there is no statistically significant difference between the two curves at 95% confidence level

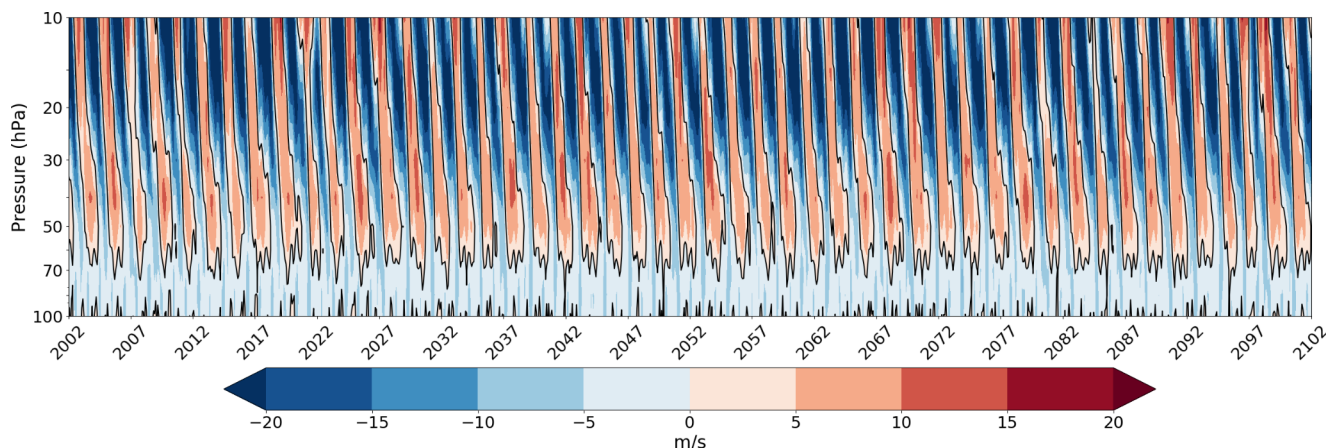## 5.2 Appendix 2. QBO in EC-EARTH3.3

See Fig. 10

Fig. 10 Vertical cross-section of monthly zonal-mean zonal wind (m/s) at the equator during the whole integration of QBOi "Experiment 2" in EC-EARTH. Black contour stands for the zero-wind line

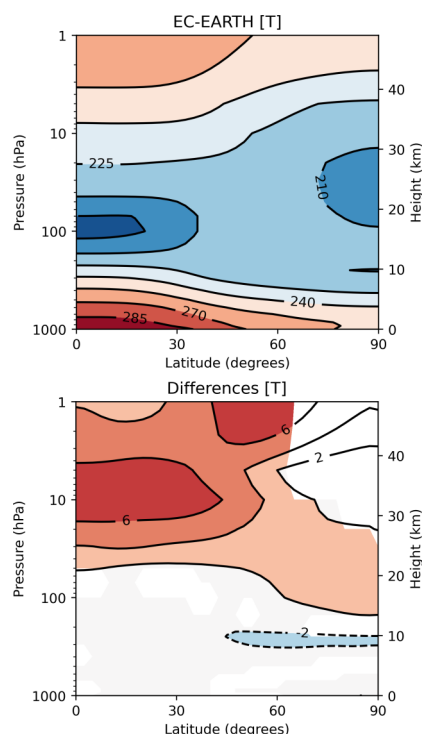## 5.3 Appendix 3. Zonal-mean temperature in transient simulations

See Fig. 11.

Fig. 11 Vertical cross-section of DJF zonal-mean temperature (K) climatology in EC-EARTH (top) and its difference with respect to ERA-Interim (bottom); to be compared with Fig. 1b,f. Model data come from three members of CMIP6 AMIP with EC-EARTH3.3 over 1979–2017 [r1, r3, r4]; available at ESGF on December 2020

5.4 Appendix 4. From EC-EARTH3.1 to EC-EARTH3.3

To complement Palmeiro et al. (2020), who focused on boreal winter variability in a previous version of the model, EC-EARTH3.1. Figure 12 shows DJF climatology of zonal-mean zonal wind and temperature in EC-EARTH3.1 using a similar model configuration (see Sect. 2 in Palmeiro et al. 2020 for details), as well as their difference with respect to ERA-Interim. The warm bias in the tropical-midlatitude stratosphere is a persistent feature in both model versions, which is largely due to the ozone radiation scheme in the atmospheric component of EC-EARTH, IFS (Hogan et al. 2017; Shepherd et al. 2018). This thermal bias is expected to be reduced in EC-EARTH4 (see Sect. 4)

On the other hand, there has been a clear improvement of the stratospheric polar vortex strength in the middle-upper stratosphere, which was largely overestimated in EC-EARTH3.1 (Fig. 12) as compared to EC-EARTH3.3 (Fig. 1e). Associated with this considerably biased westerly wind in EC-EARTH3.1, and in thermal wind balance, there is a large negative temperature bias in the upper stratosphere (Fig. 12), which is mostly absent in EC-EARTH3.3 (Fig. 1f). A too strong/too cold stratospheric polar vortex suggests a lack of dynamical variability, mainly wave activity (e.g. Charlton-Perez et al. 2013; Shaw et al. 2014). A hypothesis for this improvement is the difference of the non-orographic gravity wave (NGW) parameterization, with an increase in the launched momentum flux of these waves from sub-tropical to polar latitudes in EC-EARTH3.3 with respect to EC-EARTH3.1 (Fig. 13; see Davini et al. 2017 for details).

However, the maximum value of this launched momentum flux (GFLUXLAUN = 3.75mPa) could represent an excessive wave forcing and contribute to the negative bias of the polar vortex in the lower stratosphere (Fig. 1e), so further tuning may be advisable (see also discussion on NGW parameterization in Sect. 4)
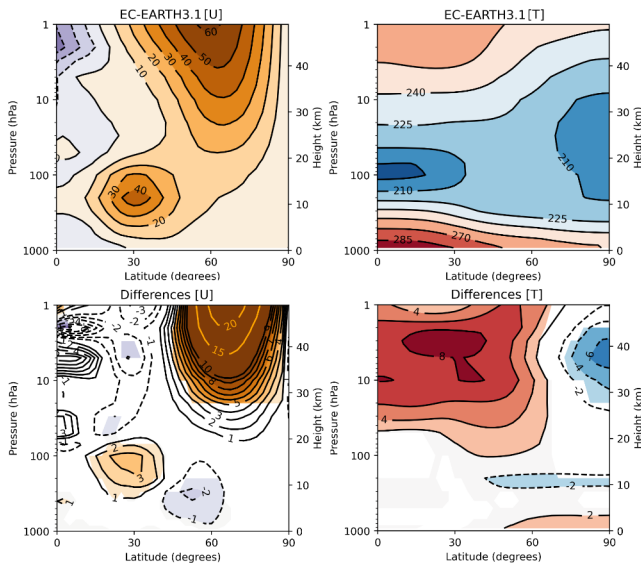
Fig. 12 Vertical cross-section of DJF zonal-mean zonal wind (m/s; left) and temperature (K; right) climatology in EC-EARTH3.1 (top) and its difference with respect to ERA-Interim (bottom); to be compared with Fig. 1**b**,**f**
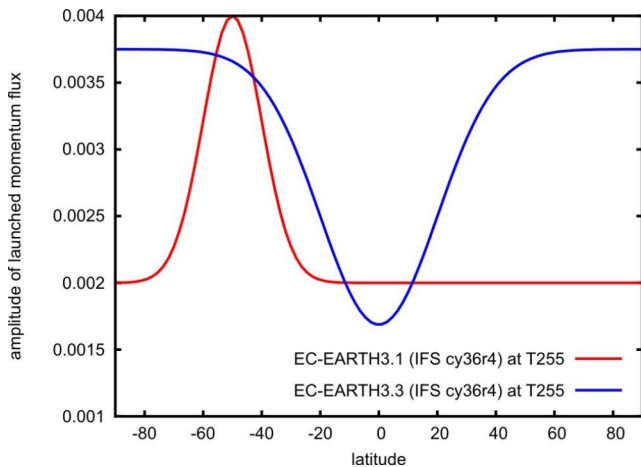
Fig. 13 Amplitude of the launched momentum flux (Pa) in the non-orographic gravity wave parameterization, depending on latitude at T255 resolution, in EC-EARTH3.1 (red) and EC-EARTH3.3 (blue)

Supplementary Information The online version contains supplementary material available at https://doi.org/10.1007/s00382-022-06368-0.

References

Abalos M, Legras B, Ploeger F, Randel WJ (2015) Evaluating the advective Brewer-Dobson circulation in three reanalyses for the period 1979–2012. J Geophys Res Atmos 120(15):7534–7554. https://doi.org/10.1002/2015JD023182

Andrews DG, Holton JR, Leovy CB (1987) Middle atmosphere dynamics (No. 40). Academic Press

Anstey JA, Shepherd TG (2014) High-latitude influence of the quasi-biennial oscillation. Quart J R Meteorol Soc 140:1–21. https://doi.org/10.1002/qj.2132

Baldwin MP et al (2001) The quasi-biennial oscillation. Rev Geophys 39:179–229

Baldwin MP, Ayarzaguena B, Birner T, Butchart N, Butler AH, Perez AJC, Domeisen DIV, Garfinkel CI, Garny H, Gerber EP, Hegglin MI, Langematz U, Pedatella NM (2021) Sudden stratospheric warmings. Rev Geophys 59:1

Beljaars A, Brown AR, Wood N (2004) A new parametrization of turbulent orographic form drag. Q J R Meteorol Soc 130:1327–1347

Berner J et al (2017) Stochastic parameterization: towards a new view of weather and climate models. Bull Am Meteorol Soc 98(3):565–588

Birner T, Bönisch H (2011) Residual circulation trajectories and transit times into the extratropical lowermost stratosphere. Atmos Chem Phys 11(2):817–827. https://doi.org/10.5194/acp-11-817-2011

Brewer AW (1949) Evidence for a world circulation provided by the measurements of helium and water vapour distribution in the stratosphere. Q J R Meteorol Soc 75:351–363

Bueh C, Nakamura H (2007) Scandinavian pattern and its climatic impact. Quart J R Meteorol Soc 133:2117–2131

Butchart N et al (2018) Overview of experiment design and comparison of models participating in phase 1 of the SPARC Quasi-Biennial Oscillation initiative (QBOi). Geosci Model Dev 11(3):1009–1032

Charlton-Perez AJ et al (2013) On the lack of stratospheric dynamical variability in low-top versions of the CMIP5models. J Geophys Res Atmos 118:2494–2505

Charlton AJ, Polvani LM (2007) A new look at stratospheric sudden warmings. Part I: climatology and modeling benchmarks. J Clim 20:449–469

Charney JG, Drazin PG (1961) Propagation of planetary- scale disturbances from the lower into the upper atmosphere. J Geophys Res 66:83–109. doi:https://doi.org/10.1029/JZ066i001p00083

Chen P, Robinson WA (1992) Propagation of planetary-waves between the troposphere and stratosphere. J Atmos Sci 49:2533–2545

Christiansen B (1999) Stratospheric vacillations in a general circulation model. J. Atmos. Sci. 56:1858–1872. https://doi.org/10.1175/1520 − 0469(1999)056,1858:SVIAGC.2.0.CO;2

Christiansen B (2005) Downward propagation and statistical forecast of the near-surface weather. J Geophys Res Atmos 110. doi:https://doi.org/10.1029/2004JD005431

Christiansen B, Yang S, Madsen MS (2016) Do strong warm ENSO events control the phase of the stratospheric QBO? Geophys Res Lett 43(19):10–489

Collins WJ et al (2017) AerChemMIP: quantifying the effects of chemistry and aerosols in CMIP6. Geosci Model Dev 10:585–607

Davini P et al (2017) Climate SPHINX: evaluating the impact of resolution and stochastic physics parameterisations in the EC-Earth global climate model. Geosci Model Dev 10(3):1383–1402

de la Cámara A, Lott F (2015) A parameterization of gravity waves emitted by fronts and jets. Geophys Res Lett 42:2071–2078

de la Cámara A, Lott F, Abalos M (2016) Climatology of the middle atmosphere in LMDz: impact of source-oriented parameterizations of gravity waves. J Adv Model Earth Syst 8:1507–1525

de la Cámara A, Albers JR, Birner T, García RR, Hitchcock P, Kinnison DE, Smith AK (2017) Sensitivity of sudden stratospheric warmings to previous stratospheric conditions. J Atmos Sci 74:2857–2877. doi:https://doi.org/10.1175/JAS-D-17-0136.1

Dee D et al (2011) The ERA-Interim reanalysis: configuration and performance of the data assimilation system. Quart J R Meteorol Soc 137:535–597

Deser C, Lehner F, Rodgers KB et al. (2020) Insights from Earth system model initial-condition large ensembles and future prospects. Nat Clim Chang 10:277–286. https://doi.org/10.1038/s41558-020-0731-2

Domeisen DI, Butler AH (2020) Stratospheric drivers of extreme events at the Earth's surface. Commun Earth Environ 1(1):1–8

Domeisen DIV, Butler AH, Charlton-Perez AJ, Ayarzagüena B, Dunn-Sigouin E, Furtado JC, Garfinkel CI, Hitchcock P, Karpechko AY, Kim H, Knight J, Lang AL, Lim EP, Marshall A, Roff G, Schwartz C, Simpson IR, Son SW, Taguchi M (2020) The role of the stratosphere in subseasonal to seasonal prediction: 2. Predictability arising from stratosphere-troposphere cou- pling. J Geophys Res Atmos 125:e2019JD030923

Döscher R et al (2022) The EC-Earth3 earth system model for the Climate Model Intercomparison Project 6. Geosci Model Dev 15:2973–3020

Dunkerton TJ(1997) The role of gravity waves in the quasi-biennial oscillation.J Geophys Res(102) D22:26,053–26,076

Dunn-Sigouin E, Shaw TA (2015) Comparing and contrasting extreme stratospheric events, including their coupling to the tropospheric circulation. J Geophys Res Atmos 120:1374–1390

Dunn-Sigouin E, Shaw TA (2018) Dynamics of Extreme Stratospheric Negative Heat Flux Events in an Idealized Model. J Atmos Sci 75:3521–3540

ECMWF (2010) IFS documentation cycle 36r1, available at https://www.ecmwf.int/en/publications/ifs-documentation

Edwards DP (1982) Solar heating by ozone in the tropical stratosphere. Quart J R Meteor Soc 108(455):253–262

Forster PMdF, Shine KP (1997) Radiative forcing and temperature trends from stratospheric ozone changes. J Geophys Res Atmos 102(D9):10841–10855

García-Serrano J, Frankignoul C, King MP, Arribas A, Gao Y, Guemas V, Matei D, Msadek R, Park W, Sanchez-Gomez E (2017) Multimodel assessment of linkages between eastern Arctic sea-ice variability and the Euro-Atlantic atmospheric circulation in current climate. Clim Dyn 49(7–8):2407–2429

Gates WL, Boyle JS, Covey C, Dease CG, Doutriaux CM, Drach RS, FiorinoM, Glecker PJ, Hnilo JJ, Marlais SM, Phillips TJ, Potter GL, Santer BD, Sperber KR, Taylor KE, Williams DN (1999) An overview of the results of the atmospheric model intercomparison project (AMIP I). Bull Am Meteorol Soc 80:29–55

Gerber EP, Butler A, Calvo N, Charlton-Perez AJ, Giorgetta M, Manzini E, Perlwitz J (2012) Assessing and understanding the impact of stratospheric dynamics and variability on the earth system. Bull Am Meteorol Soc 93:845–859. doi:https://doi.org/10.1175/BAMS-D-11-00145.1

Gerber EP et al (2010) Stratosphere-troposphere coupling and annular mode variability in chemistry-climate models. J Geophys Res 115. doi:https://doi.org/10.1029/2009JD013770. :D00M06

Haarsma R, Acosta M, Bakhshi R, Bretonniére PAB, Caron LP, Castrillo M, Corti S, Davini P, Exarchou E, Fabiano F, Fladrich U, Fuentes Franco R, García-Serrano J, von Hardenberg J, Koenigk T, Levine X, Meccia V, van Noije T, van den Oord G, Palmeiro FM, Rodrigo M, Ruprich-Robert Y, Le Sager P, Tourigny E, Wang S, van Weele M, Wyser K (2020) Highresmip versions of EC-Earth: EC-Earth3p and EC-Earth3p-hr. Description, model performance, data handling and validation. Geosci Model Dev Discuss. https://doi.org/10.5194/gmd-2019-350

Hardiman SC, Butchart N, O'Connor FM, Rumbold ST (2017) The Met Office HadGEM3-ES chemistry-climate model: evaluation of stratospheric dynamics and its impact on ozone. Geosci Model Dev 10:1209–1232

Harvey VL, Hitchman MH(1996) A climatology of the Aleutian High. J Atmos Sci 53:2088–2101. https:// doi. org/ 10. 1175/ 1520 − 0469(1996) 053% 3c2088: ACOTAH% 3e2.0. CO;2

Harvey VL, Pierce RB, Hitchman MH (2002) A climatology of stratospheric polar vortices and anticyclones. J Geophys Res 107(D20):4442 https:// doi. org/ 10. 1029/ 2001J D0014 71

Haase S, Matthes K (2019) The importance of interactive chemistry for stratosphere-troposphere coupling. Atmos Chem Phys 19:3417–3432

Hazeleger W et al (2010) EC-Earth: a seamless earth-system prediction approach in action. Bull Am Meteorol Soc 91:1357–1363. doi:https://doi.org/10.1175/2010BAMS2877.1

Hazeleger W et al (2012) EC-Earth V2.2: Description and validation of a new seamless earth system prediction model. Clim Dyn 39:2611–2629

Highwood EJ, Hoskins BJ (1998) The tropical tropopause. Quart J Roy Meteor Soc 124:1579–1604

Hogan RJ, Bozzo A (2018) A flexible and efficient radiation scheme for the ECMWF model. J Adv Model Earth Sy 10:1990–2008. https://doi.org/10.1029/2018MS001364

Hogan RJ, Ahlgrimm M, Balsamo G, Beljaars A, Berrisford P, Bozzo A, Di Giuseppe F, Forbes RM, Haiden T, Lang S, Mayer M, Polichtchouk I, Sandu I, Vitart F, Wedi N(2017) Radiation in numerical weather prediction. ECMWF Tech Memo 816, Reading, 49 pp

Holton JR, Tan HC (1980) The influence of the equatorial quasi-biennial oscillation on the global circulation at 50 mb. J Atmos Sci 37:2200–2208

Holton JR, Haynes PH, McIntyre ME, Douglass AR, Rood RB, Pfister L (1995) Stratosphere–troposphere exchange. Rev Geophys 33:403–439

Kidston J, Scaife AA, Hardiman SC, Mitchell DM, Butchart N, Baldwin MP, Gray LJ (2015) Stratospheric influence on tropospheric jet streams, storm tracks and surface weather. Nat Geosci 8:433–440

Kodera K, Kuroda Y, Pawson S (2000) Stratospheric sudden warmings and slowly propagating zonal-mean zonal wind anomalies. J Geophys Res 105(12):351–12359

Kuroda Y, Kodera K (1999) Role of planetary waves in the stratosphere–troposphere coupled variability in the Northern Hemisphere winter. Geophys Res Lett 26:2375–2378

Limpasuvan V, Hartmann DL, Thompson DWJ, Jeev K, Yung YL (2005) Stratosphere-troposphere evolution during polar vortex intensification. J Geophys Res 110. https://doi.org/10.1029/2005JD006302

Liu Y, Wang L, Zhou W, Chen W (2014) Three Eurasian teleconnection patterns: spatial structures, temporal variability, and associated winter climate anomalies. Clim Dyn 42:2817–2839

Manzini E et al (2014) Northern winter climate change: Assessment of uncertainty in CMIP5 projections related to stratosphere-troposphere coupling. J Geophys Res Atmos 119(13):7979–7998

Lott F, Miller MJ (1997) A new subgrid-scale orographic drag parametrization: its formulation and testing. Q J R Meteorol Soc 123:101–127

Matsuno T (1970) Vertical propagation of stationary planetary waves in the winter Northern Hemisphere. J Atmos Sci 27:871–883

Matsuno T (1971) A dynamical model of the stratospheric sudden warming. J Atmos Sci 28:1479–1494

Morgenstern O et al (2017) Review of the global models used within phase 1 of the Chemistry-Climate Model Initiative (CCMI). Geosci Model Dev 10:639–671

Newman PA, Nash ER (2000) Quantifying the wave driving of the stratosphere. J Geophys Res Atmos 105(D10):12485–12497

Nigam S, DeWeaver E (2003) Stationary waves (orographic and thermally forced). In: Holton JR, Pyle J, Curry JA (eds) Encyclopedia of atmospheric sciences. Academic Press, Cambridge, pp 2121–2137

Nishii K, Nakamura H, Miyasaka T (2009) Modulations in the planetary wave field induced by upward propagating Rossby wave packets prior to stratospheric sudden warming events: a case-study. Quart J R Meteor Soc 135:39–52. doi:https://doi.org/10.1002/qj.359

Orr A, Bechtold P, Scinocca J, Ern M, Janiskova M (2010) Improved middle atmosphere climate and forecasts in the ECMWF model through a non-orographic gravity wave drag parameterization. J Clim 23:5905–5926

Palmeiro FM, García-Serrano J, Bellprat O et al(2020) Boreal winter stratospheric variability in EC-EARTH: High-Top versus Low-Top. Clim Dyn 54:3135–3150. https:// doi. org/ 10. 1007/ s00382-020-05162-0

Palmeiro FM, Garcia-Serrano J, Ruggieri P, Batté L, Gualdi S(2022) On the influence of ENSO on sudden stratospheric warmings. Clim Dyn (submitted)

Plumb RA (1985) On the three-dimensional propagation of stationary waves. J Atmos Sci 42(3):217–229 https://doi.org/10.1175/1520-0469(1985)042(0217:OTTDPO)2.0.CO;2

Plumb RA (2002) Stratospheric Transp J Meteor Soc Japan 80:793–809

Polichtchouk I, Stockdale TN, Bechtold P, Diamantakis M, Malardel S, Sandu I, Vana F, Wedi N(2019) Control on stratospheric temperature in IFS: resolution and vertical advection. ECMWF Tech Memo 847, Reading, 36 pp

Portal A, Ruggieri P, Palmeiro FM, García-Serrano J, Domeisen DIV, Gualdi S (2022) Seasonal prediction of the boreal winter stratosphere. Clim Dyn doi. https://doi.org/10.1007/s00382-021-05787-9

Richter JH, Butchart N, Kawatani Y, Bushell AC, Holt L, Serva F, … Yukimoto S(2020) Response of the Quasi-Biennial Oscillation to a warming climate in global climate models. Quart J R Meteor Soc

Saurral RI, Merryfield WJ, Tolstykh MA, Lee W-S, Doblas-Reyes FJ, García-Serrano J, Massonnet F, Meehl GA, Teng H (2021) A dataset for intercomparing the transient behavior of dynamical model-based subseasonal to decadal climate predictions. J Adv Model Earth Syst. https://doi.org/10.1029/2021MS002570

Scinocca JF (2003) An accurate spectral nonorographic gravity wave drag parameterization for general circulation models. J Atmos Sci 60(4):667–682

Shaw TA, Perlwitz J (2013) The life cycle of Northern Hemisphere downward wave coupling between the stratosphere and troposphere. J Clim 26:1745–1763

Shaw TA, Perlwitz J, Weiner O (2014) Troposphere–stratosphere coupling: links to North Atlantic weather and climate, including their representation in CMIP5 models. J Geophys Res Atmos 119:5864–5880. doi: https://doi.org/10.1002/2013JD021191

Shepherd TG (2007) Transport in the middle atmosphere. J Meteor Soc Japan 85B:165–191

Shepherd TG, Polichtchouk I, Hogan RJ, Simmons AJ(2018) Report on Stratosphere Task Force. ECMWF Tech Memo 824, Reading, 32 pp

Sigmond M, Scinocca FJ, Kharin V, Shepherd T (2013) Enhanced seasonal forecast skill following stratospheric sudden warmings. Nat Geosci 6:98–102

Simpson IR, Bacmeister J, Neale RB, Hannay C, Gettelman A, Garcia RR, … Richter JH(2020) An evaluation of the large-scale atmospheric circulation and its variability in CESM2 and other CMIP models. J Geophys Res: Atmos 125(13): e2020JD032835

Smith KL, Kushner PJ (2012) Linear interference and the initiation of extratropical stratosphere–troposphere interactions. J Geophys Res 117:D13107. https://doi.org/10.1029/2012JD0175 87

Smith D et al (2019) Robust skill of decadal climate predictions. npj Clim Atmos Sci 2:1–10. https://doi.org/10.1038/s41612-019-0071-y

Smoliak BV, Wallace JM (2015) On the leading patterns of Northern Hemisphere sea level pressure variability. J Atmos Sci 72(9):3469–3486

Stockdale T, Kim YH, Anstey JA, Palmeiro FM, Butchart N, Scaife AA, Andrews M, Bushell AC, Dobrynin M, García-Serrano J, Hamilton K, Kawatani Y, Lott F, McLandress C, Naoe H, Osprey S, Pohlmann H, Scinocca J, Watanabe S, Yoshida K, Yukimoto S (2022) Prediction of the quasi-biennial oscillation with a multi-model ensemble of QBO-resolving models. Quart J R Meteorol Soc. https://doi.org/10.1002/qj.3919

Takaya K, Nakamura H (2008) Precursory changes in planetary wave activity for midwinter surface pressure anomalies over the Arctic. J Meteorol Soc Jpn Ser II 86(3):415–427

Tripathi OP, Baldwin M, Charlton-Perez AJ, Charron M, Eckermann SD, Gerber E, Harrison RG, Jackson DR, Kim B-M, Kuroda Y, Lang A, Mahmood S, Mizuta R, Roff G, Sigmond M, Son SW (2015) The predictability of the extratropical stratosphere on monthly time-scales and its impact on the skill of tropospheric

forecasts. Quart J R Meteorol Soc 141:987–1003. doi: https://doi.org/10.1002/qj.2432

Vallis GK (2017) Atmospheric and oceanic fluid dynamics. Cambridge University Press, Cambridge

van Noije T et al (2021) EC-Earth3-AeroChem: a global climate model with interactive aerosols and atmospheric chemistry participating in CMIP6. Geosci Model Dev 149:5637–5668

Woollings T, Blackburn M (2012) The North Atlantic jet stream under climate change and its relation to the NAO and EA patterns. J Clim 25:886–902

Wyser K et al (2020) On the increased climate sensitivity in the EC-Earth model from CMIP5 to CMIP6. Geosci Model Dev 138:3465–3474

Zappa G, Shaffrey LC, Hodges KI (2013) The ability of CMIP5 models to simulate North Atlantic extratropical cyclones. J Clim 26:5379–5396

Perlwitz J, Graf HF (1995) The statistical connection between tropospheric and stratospheric circulation of the Northern Hemisphere in winter. J Clim 8:2281–2295

Gerber, EP and Manzini, E (2016) The Dynamics and Variability Model Intercomparison Project (DynVarMIP) for CMIP6: assessing the stratosphere–troposphere system. Geosci Model Dev 9:3413–3425. https://doi.org/10.5194/gmd-9-3413-2016, 2016.